ADVANCED FUNCTIONAL MATERIALS
www.afm-journal.de

Stabilization of Amorphous Calcium Carbonate with Nanofibrillar Biopolymers

*David C. Bassett, Benedetto Marelli, Showan N. Nazhat, and Jake E. Barralet**

Calcium carbonate is the most abundant biomineral that is biogenically formed with a vast array of nano and microscale features. Among the less stable polymorphs present in mineralized organisms, the most soluble, amorphous calcium carbonate (ACC), formed in chitin exoskeletons of some crustacea, is of particular interest since aqueous stability of isolated ACC is limited to a few hours in the absence of polyanions or magnesium. Here the influence of a selection of biopolymer gels on the mineralization of calcium carbonate is investigated. Mineralization is achieved in all biopolymers tested, but is particularly abundant in collagen hydrogels, in which a significant proportion of the calcium carbonate (≈18%) is found to be amorphous. In dense collagen gels, this amorphous fraction does not crystallize for up to six weeks in deionized water at room temperature. The reason why collagen in particular should stabilize this phase remains obscure, although the results suggest that the fiber diameter, fiber spacing, and the amphoteric nature of collagen fibers are important. Upon immersion in phosphate containing solutions, the calcium carbonate present within the collagen hydrogels is readily converted to carbonated hydroxyapatite, enabling the formation of a stiff bone-like composite containing 78 wt% mineral, essentially equivalent to cortical bone.

1. Introduction

Hard tissues are composites comprised of cell-formed organic matrices and amorphous or crystalline inorganic minerals. The two principle organic matrices that provide skeletal support for animals are the polysaccharide chitin and the protein collagen. Both of these polymers are nanofibrous and contain proteins and polysaccharides that are thought to play key roles in providing two or three dimensional templates onto or into which mineral forms. Indeed, the chitin-protein system of crustacea and mollusks has been proposed to be a reverse analogue of the collagen-polysaccharide skeletal system in vertebrates.[1] As such, chitin and collagen have been proposed as universal templates for biomineralization[2] and the recent discovery[3] of collagenous proteins in fungi has added weight to the theory of a common evolutionary ancestry for these extracelluar matrix (ECM) components.

There are three main ways in which organic matrices control inorganic mineralization *in vivo*: 1) physical confinement within the organic structure to allow growth of non-equilibrium morphology, 2) chemical interaction to influence polymorph selection and oriented nucleation or 3) a combination of the two.[4] All three approaches have instructed biomimetic and bioinspired studies *in vitro* to both elucidate biological mineralization mechanisms and to form functional materials with interesting properties, particularly at the nanoscale, via low temperature, environmentally benign pathways.[5]

Biogenic minerals may occur in the form of non-thermodynamically stable polymorphs or amorphous materials that are templated and stabilized by the organic matrix, such as amorphous calcium carbonate (ACC) found in crustacean chitin exoskeletons,[6] and to date there is no satisfactory explanation for how this occurs. Amorphous calcium phosphate (ACP) has also been implicated as a precursor phase to hydroxyapatite in both invertebrate[7] and vertebrate hard tissues.[8] While the presence in vertebrates is still a subject of debate,[9] the lack of diffraction, inherent instability and presence of other phases make characterization problematic. Attempts at remineralizing chemically demineralized hard tissue matrices *in vitro* have resulted in formations that closely resemble the original form, but do not exactly replicate it.[10] We are not aware of any reports on successful remineralization of stable amorphous phases in demineralized matrices.

Non-biogenic ACC is inherently unstable in aqueous conditions, crystallizing within minutes at room temperature. Within mineralizing organisms it is stabilized by the extracellular matrix or it functions as a precursor to other crystalline phases.[11] The roles of biological matrices in eliciting stability over this highly reactive compound have been widely investigated, inspired particularly from marine organisms containing ACC;[12] macromolecules containing glycine, glutamate, phosphate or polysaccharide groups and inorganic magnesium ions have been identified as having a particular ability in this regard.[13] Recently two prominent phosphate containing

Dr. D. C. Bassett, Prof. S. N. Nazhat, Prof. J. E. Barralet
Faculty of Dentistry
McGill University
Montreal, QC, H3A 2B2, Canada
E-mail: jake.barralet@mcgill.ca
Dr. B. Marelli, Prof. S. N. Nazhat
Department of Mining and Materials Engineering
McGill University
Montreal, QC, H3A 2B2, Canada

DOI: 10.1002/adfm.201103144

biomolecules, phosphoenolpyruvate and 3-phosphoglycerate, have been identified as having a significant stabilizing effect.[14] *In vitro*, other molecules and proteins not previously associated with calcium carbonate biomineralization such as phytic acid[13] and whole serum[15] have also been shown to inhibit crystallization of ACC particularly strongly when present in solution.

Here we studied the ability of several biomaterial hydrogels to template the formation of calcium carbonate and assessed their ability to stabilize ACC in order to determine whether simple confinement in a gel was indeed sufficient for ACC stabilization. We made the highly unexpected discovery that type I collagen appeared to have an innate ability to stabilize ACC for at least six weeks in ion-free water, something that has never been achieved to date except in biological tissues. The effects of fibril density and precipitation milieu are reported. Furthermore the calcium carbonate remained highly reactive and could rapidly be converted to hydroxyapatite at room temperature forming a homogeneously mineralized (78 wt%) collagen-apatite composite without an accumulation of mineral at the matrix surface often observed in *in vitro* supersaturated mineralizing solutions. This demonstrates the potential of this approach for the formation of readily mineralizable hard tissue scaffold materials that could be applied through minimally invasive techniques, (since the ACC loaded collagen gel was still soft and pliable prior to phosphate conversion). Our work points to the similarity in nanostructure of collagen and chitin being a key factor in their ability to stabilize amorphous calcium minerals.

2. Results

2.1. Formation of Calcium Carbonate with Biopolymers

When biopolymers were present in precipitation solutions, the quantity of mineral formed ranged from ~16–75 wt% (**Table 1**). **Figure 1** depicts the morphology of the mineralized agarose, alginate, chitosan and fibroin surfaces observed by SEM and accompanying FTIR and XRD data. Dispersed mineral deposits as confirmed by EDX (not shown) were formed on the surface of agarose gels (Figure 1a). FTIR spectra of the as made gel showed the characteristic bands at 1070 and 930 cm^{-1} corresponding to the 3,6-anhydro-galactose bridges. The spectrum of the mineralized gel presented clear increases in absorbances at 1410, 866 and 711 cm^{-1}, which were assigned to the ν_3, ν_2 and ν_4 modes respectively of calcium carbonate in the form of calcite (see **Table 2**).[14] The formation of calcite was confirmed by XRD, which also revealed the presence of a small amount of calcium hydroxide $Ca(OH)_2$ in the gel. This was also detected by FTIR (strong absorption peak at 3128, 3047 and 2818 cm^{-1}, data not shown). For alginate gels (Figure 1b), SEM analysis showed that the minerals formed were integrated in the microstructure of the polysaccharide, and the two phases were not microscopically distinguishable. FTIR analysis of the as made gel showed the typical IR absorption of the polysaccharide at 1596 cm^{-1} due to the stretching of the carboxyl groups, at 1412 cm^{-1} due to the asymmetric CO_2^- stretch, at 1385 and 1347 cm^{-1} due to the C-O and O-H vibrations, and at 1297, 1081 and 1021 cm^{-1} due to the C-O-C asymmetric stretch. The FTIR spectrum of the mineralized sample was characterized by increased absorbances at 1410, 866 and 711 cm^{-1}. XRD confirmed the presence of calcite, however a large fraction of $Ca(OH)_2$ was also found. For chitosan gels (Figure 1c), SEM revealed crystals of various shapes within the polymeric glucosamine. The spectrum of the as made sample was characterized by typical absorptions at 1647 cm^{-1} assigned to the amide I, at 1560 cm^{-1} assigned to the NH bending (amine and amide II), at 1411 cm^{-1} assigned to CH_2 bending, at 1380 cm^{-1} due to CH_3 wagging, at 1150 cm^{-1} assigned to C-O-C and C-N stretch and at 1026 cm^{-1} due to skeletal vibrations of C-O stretching. As for the other polysaccharides previously investigated, the FTIR spectrum of the mineralized sample was characterized by an increased absorbance at 1410, 866 and 711 cm^{-1} indicating the formation of calcium carbonate. This result was corroborated with XRD analysis. For electrospun fibroin (Figure 1d), SEM revealed the nanofibrillar form of the protein, with sporadic nucleation of minerals within the matrix. FTIR spectra of the as made and mineralized samples showed the typical antiparallel β-sheet structure of the protein characterized by the amide I, II and III absorptions at 1691 and 1621, 1550 and 1243 cm^{-1}, respectively. The marked increase in absorbance at 1410, 866 and 711 cm^{-1} in the mineralized sample indicated the formation of calcite, also confirmed by XRD. SEM images (Figure 1) depict the typical appearance of the washed surfaces of the biopolymers.

In all biopolymer gels tested, the pH of the calcium chloride solution during the gas diffusion mediated mineralization was measured at 0, 2, and 72 hours reaction time and was found to be pH 5.5, rising to 9.4–9.6 before falling slightly to 9.1–9.2 respectively. This is consistent with our previous report using this system in which pH was measured constantly.[5d]

Table 1. Amounts of inorganic mineral formed in biopolymers as measured by TGA and the amorphous fraction of $CaCO_3$ as calculated from FTIR through the ν_2/ν_4 absorbance ratios.

Biopolymer	Mineral [wt%]	ACC/Calcite [%]	ACC [wt%]	ACC [wt%] after 6 weeks in water
Agarose	16.0	0.8 ± 0.5	0.13	–
Alginate	33.4	1 ± 0.7	0.33	–
Chitosan	36.2	0.9 ± 0.5	0.33	–
Fibroin	15.9	0.5 ± 0.4	0.08	–
14.1 wt% Collagen	72.7	9 ± 1.8	6.5	5.0
0.2 wt% Collagen	74.6	18 ± 1.3	13.4	1.5

2.2. Formation of Calcium Carbonate in Collagen Gels

TGA revealed a much higher content of mineral formed in 0.2 wt% and 14.2 wt% collagen gels (~75 wt%, Table 1) than the other biopolymers. Also, DSC analysis of 0.2 wt% collagen revealed an additional weak exothermic peak at 327 °C which is attributable to the crystalline transition of ACC[17] (See Supporting Information, Figure S1 & S2), however the additional possibility of intrafibrillar mineralization affecting the thermal degradation of collagen cannot be discounted.[18] This peak was not found in any of the other hydrogels and by comparison

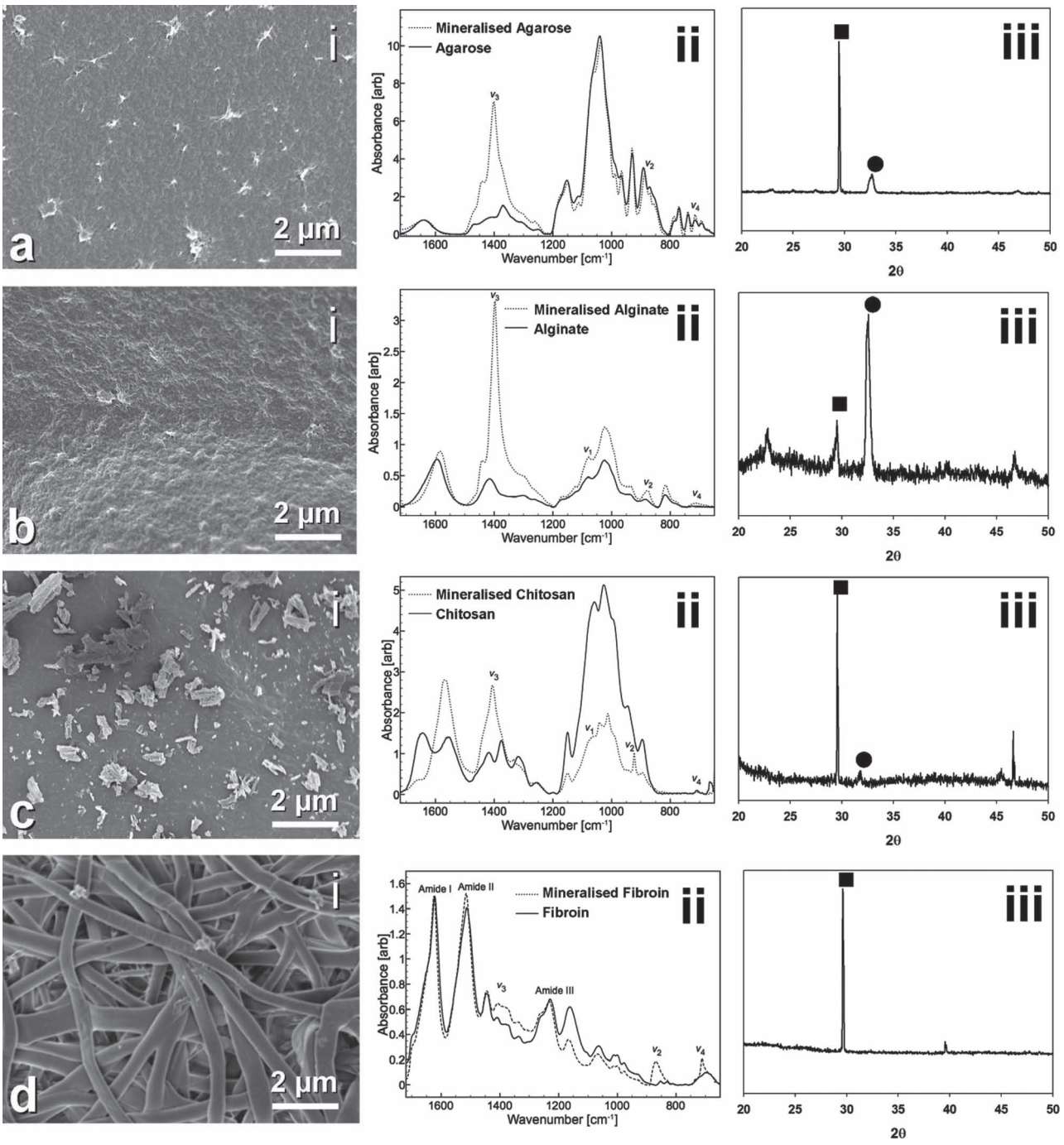

Figure 1. SEM images and accompanying FTIR and XRD traces following calcium carbonate mineralization in four biopolymers. a) Mineralization of agarose: i) SEM revealed no particular features in the gel, with sporadic presence of crystals (lighter grey). ii) FTIR analysis showed the formation of calcite in the gel, since the CO_3^{2-} v_3, v_2, v_4 resonances were centered at 1390, 866, and 712 cm^{-1}, respectively. iii) XRD analysis confirmed the FTIR results and revealed the presence of calcite (■) and $Ca(OH)_2$ (●) phases in the gel. b) Alginate: i) SEM revealed no particular features on the surface of the gel. Crystals were incorporated in the biopolymeric matrix and were not distinguishable in the image. ii) FTIR and iii) XRD analyses revealed the presence of calcite (■) and $Ca(OH)_2$ (●). c) Mineralization of chitosan: i) SEM showed poorly formed microcrystals in the gel. ii) FTIR revealed the presence of calcite, which was corroborated by iii) XRD analysis. d) Mineralization of electrospun fibroin. i) SEM revealed the nanofibrillar form of the electrospun fibroin, with sporadic deposition of poorly formed crystals (lighter grey). ii) FTIR indicated the presence of calcite, as was also supported by iii) XRD analysis.

with amorphous-crystalline calcium carbonate samples of known composition, the limit of detection for ACC by TGA was 5 wt% (Figure S1e). However, FTIR did indicate the presence of ACC in all of the biopolymer gels as determined from the ratio of the CO_3^{2-} v_2/v_4 absorbance[19] which was also calibrated with amorphous and crystalline calcium carbonate mixtures

Table 2. Main absorbance of carbonate species in the IR spectrum.

CO_3^{2-} peak	Vibration	Notes
1390 [cm^{-1}]	ν_3 asymmetric stretch in plane	Absorbance in the 1650–1300 [cm^{-1}] range, split in three main peaks
1081 [cm^{-1}]	ν_1 symmetric stretch in plane	Only present in amorphous $CaCO_3$; forbidden in rhombohedral crystals
874 [cm^{-1}]	ν_2 symmetric bend out-of-plane	Strong
713 [cm^{-1}]	ν_4 asymmetric bend in plane	Absent in amorphous $CaCO_3$

(Figure S1b). The ACC fraction in agarose, alginate, chitosan and fibroin was very low (0.2–1.7%), but the amorphous content in both 0.2 wt% and 14.2 wt% collagen gels was much higher (~9% and 18% respectively, equating to nearly 7 and 14 wt% of the total material), (Table 1). SEM analysis of the collagen gels before and after mineralization confirmed the abundant formation of inorganic mineral present throughout the biopolymer gel matrix and closely associated with the collagen fibers (**Figure 2**). These deposits did not have crystalline morphological features and were coarser in 0.2 wt% collagen compared with 14.1 wt% collagen when observed at high magnification. In both cases the length scale of the deposits were typical for those found for ACC (<1 μm c.f. Figure S1c) and the characteristic banding structure of the collagen fibers was not discernable in mineralized samples, indicating coating of the fibers with mineral. MicroCT revealed homogeneous mineralization throughout both collagen gels with sporadic areas of high density mineral (**Figure 3**a,b). FTIR and XRD confirmed the major crystalline phase to be calcite, although a small amount of $Ca(OH)_2$ was detected in 0.2 wt% collagen samples (Figure 3c,d).

2.3. Formation and Stability of ACC with Collagen

The time dependent ACC content (as calculated from FTIR ν_2/ν_4 absorbance ratio, Supporting Information Figure S1b.) for calcium carbonate precipitation in 0.2 wt% collagen gels is shown in **Figure 4**. ACC was present and stable in the gel throughout the mineralization process. The ratio recorded decreased as a function of time, indicating a higher proportion of amorphous content at early stages of formation. However, when expressed as the weight percent of total mineral, the content of ACC remained largely unchanged with time, while the total amount of mineral increased. This indicates that ACC was initially formed and crystalline calcium carbonate was deposited later.

To investigate the role of the chemical environment on the formation of calcium carbonate and stabilization of ACC, the addition of the major amino acids of collagen (ALA, ARG, GLY, PRO) at high concentration (10 wt% with respect to hydrogel) to hydrogels of chitosan and collagen did not produce any statistically significant difference ($p > 0.05$) in the amount of ACC formed in the gels. Additionally, since magnesium is known

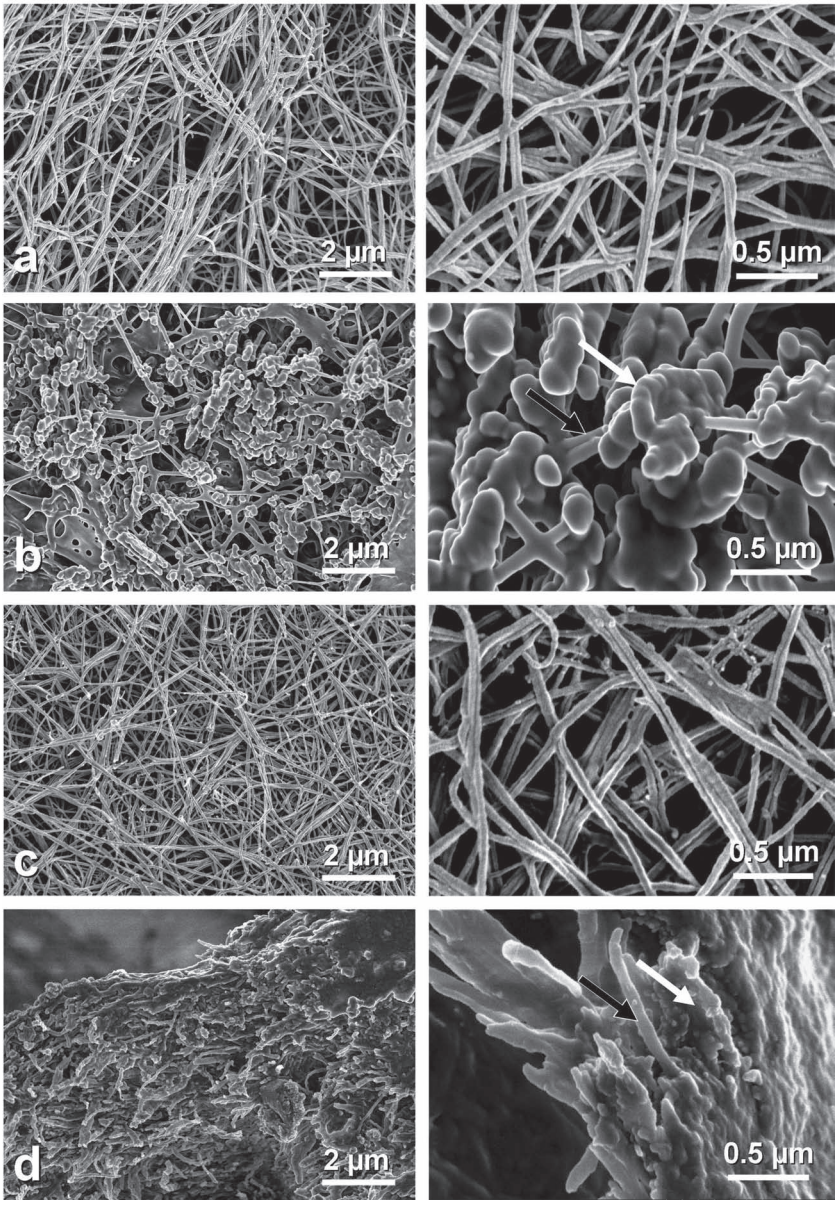

Figure 2. SEM images of 0.2 wt% collagen gel as made (a) and mineralized (b); 14.1 wt% collagen gel as made (c) and mineralized (d). In both as made gels the collagen fibers were clearly visible, with characteristic banding structure evident at high magnification. In mineralized gels, deposits (white arrows) were formed homogenously on and between collagen fibrils (black arrow), in which a banding texture was not visible and appeared slightly thicker than native fibrils.

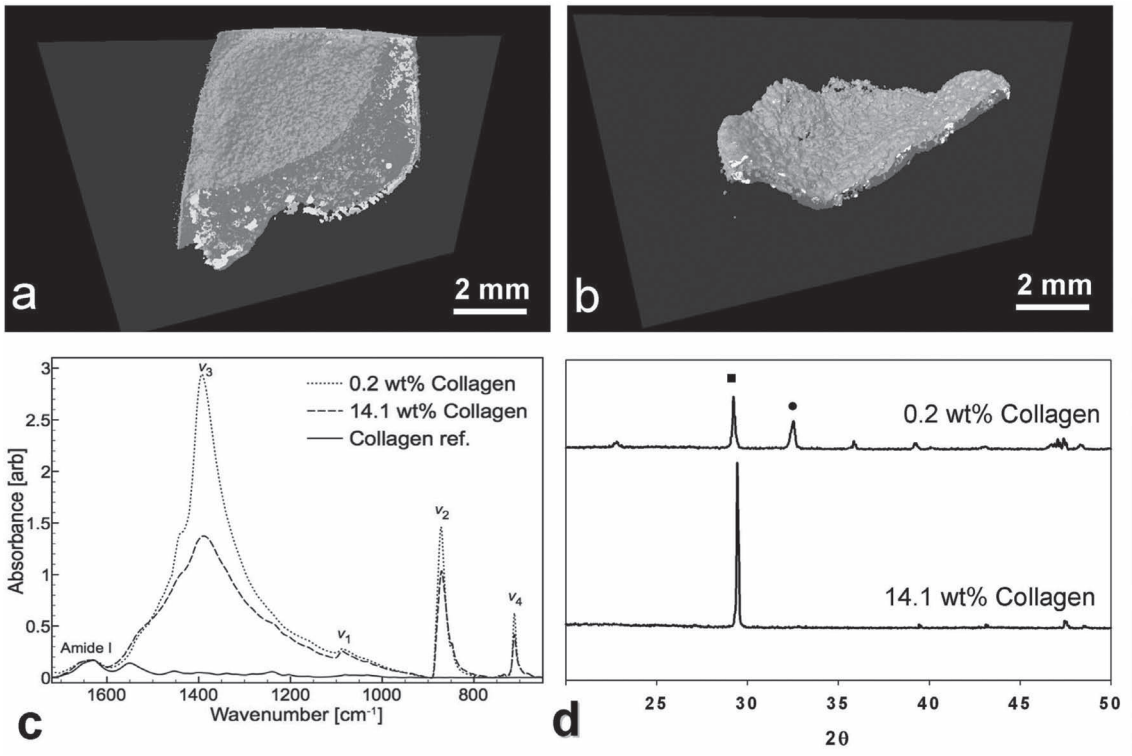

Figure 3. MicroCT 3D reconstructions of the mineral phase within 0.2 wt% (a) and 14.1 wt% (b) collagen gels showed abundant mineralization throughout the materials (highlighted in light grey) with areas of dense mineral deposits (highlighted in white). c) FTIR analysis of mineralized 0.2 and 14.1 wt% collagen gels compared to as made collagen gel. Calcite and amorphous calcium carbonate were identifiable as the ν_3, ν_1, ν_2, ν_4 resonances were centered at 1390, 1061, 866 and 712 cm^{-1}, respectively. 0.2 wt% collagen gels had an increased ν_2/ν_4 absorbance ratio when compared to the 14.1 wt% gels, indicating a higher amount of amorphous calcium carbonate. d) XRD of 0.2 and 14.1 wt% collagen gels, indicated the formation of calcite (■) within the collagen gels, and also the presence of $Ca(OH)_2$ (●) in 0.2 wt% collagen.

to influence ACC stability and because DMEM containing magnesium was used in the preparation of collagen hydrogels, DMEM was replaced by magnesium-free PBS. The percentage of ACC formed in collagen gels in the absence of magnesium was not significantly different ($p > 0.01$) to that formed in normal DMEM prepared gels. However, when either basic or acidic fuchsine was added to the collagen solution, which bind with positively or negatively charged groups respectively, ACC formation was prevented altogether, and only calcite was found by FTIR and XRD (data not shown). SEM revealed that the collagen banding structure was clearly visible when either basic or acidic fuchsine was added, however acidic fuchsine resulted in smaller calcite crystals than basic fuchsine (see Supporting Information, Figure S3).

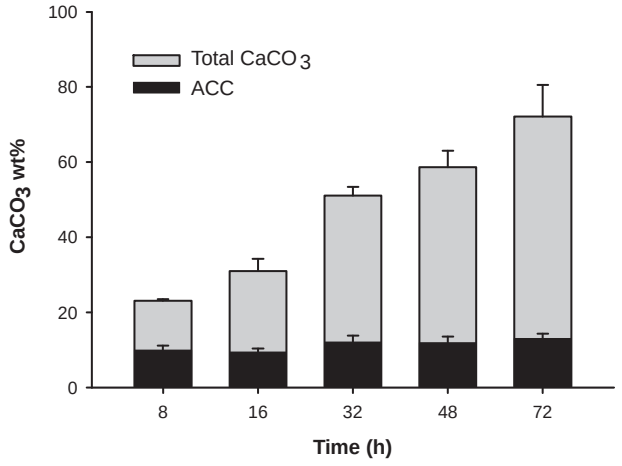

Figure 4. The total amount of $CaCO_3$ formed with time in 0.2 wt% collagen gels as determined by thermogravimetric analysis (gray bars), and the relative amount of ACC present (black bars) as determined by FTIR ν_2/ν_4 absorbance ratio. The total amount of mineral formed increased with time up to 72 h, while the relative amount of ACC present did not significantly increase over the same time period.

To determine stability of the ACC content of the collagen gels, fully mineralized samples were immersed in DI water. After 6 weeks of immersion 1.5 wt% and 5.0 wt% ACC (as calculated from FTIR ν_2/ν_4 absorbance ratio and TGA analysis) remained in the 0.2 wt% and 14.1 wt% collagen gels respectively (Table 1).

2.4. Conversion of Calcium Carbonate to Calcium Phosphate

Following immersion in a solution of sodium phosphate for 12 h, the $CaCO_3$ in both 0.2 and 14.1 wt% collagen gels transformed entirely into poorly crystalline carbonated hydroxyapatite, as determined by FTIR (increased phosphate (1112, 1075 and 1015 and 980 cm^{-1}) and carbonate (1400 and 872 cm^{-1})

Table 3. Amounts of mineral formed upon conversion to hydroxyapatite in 0.2 and 14.1 wt% collagen gels as measured by TGA and mineralized volume fraction in phosphorylated 0.2 and 14.1 wt% collagen gels as measured by microCT 3D analysis.

Collagen gel	Hydroxyapatite [wt%]	Mineralized volume fraction
0.2 wt%	78	0.85 ± 0.07
14.1 wt%	56	0.92 ± 0.04

absorptions) and XRD. A large amount of apatite mineral was found to have been deposited (up to 78 wt% of the dry gel as measured by TGA). MicroCT imaging determined the mineralized collagen volume fraction to be 85% and 92% for 0.2 wt% and 14.1 wt% gels, respectively (**Table 3**) and was homogeneous throughout the sample (**Figure 5**). Interestingly, the morphology of the HA was different although the crystallinity was similar. The crystals present in the high density gel had a plate-like morphology typical of *in vitro* mineralization from supersaturated solutions but in the low density gel individual crystallites were not discernible.

3. Discussion

By examining the ability of several biopolymers to template the formation of calcium carbonate, we found that calcite formed in all of the materials tested. The amount of calcium carbonate

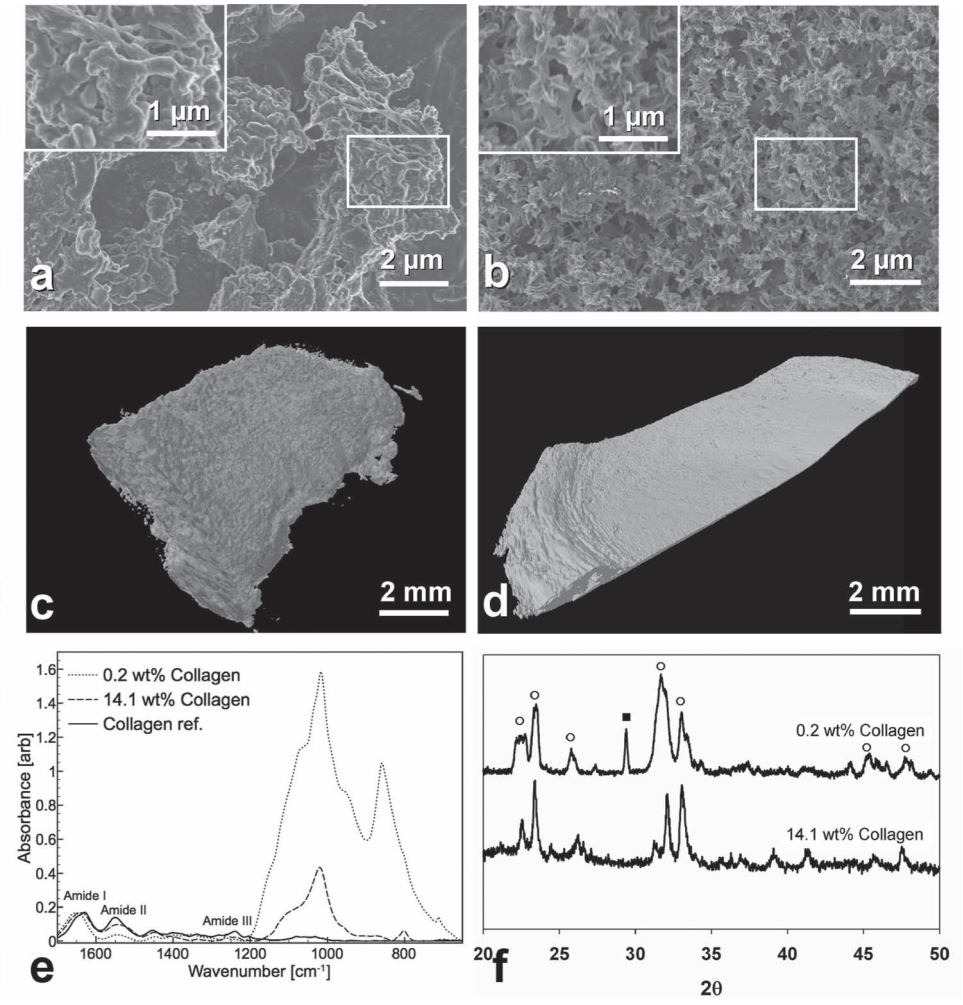

Figure 5. Morphological and chemical characterization of calcium carbonate to calcium phosphate conversion in 0.2 and 14.1 wt% collagen gels. a) SEM image of 0.2 wt% collagen gels showed the formation of minerals on the collagen fibrils b) SEM image of 14.1 wt% collagen gels showing abundant mineral formation in the interfibrillar space. Insets in (a,b) are high magnifications of the indicated areas. c) MicroCT 3D reconstruction of the mineral phase within 0.2 wt% collagen gel showed mineralization (highlighted in light grey) throughout the gel. d) MicroCT 3D reconstruction of the mineral phase within 14.1 wt% collagen gel. The minerals were formed homogenously throughout both gels. e) FTIR spectra of mineralized 0.2 and 14.1 wt% collagen gels compared to as made collagen gel (labeled as collagen ref.). While calcite was still present in the gels, carbonated hydroxyapatite was formed both in 0.2 and 14.1 wt% collagen gels. The increased phosphate (1112, 1075 and 1015 and 980 cm^{-1}) and carbonate (1400 and 872 cm^{-1}) absorptions in 0.2 wt% gels when compared to the 14.1 wt% counterpart was an indication of the higher level of mineralization achieved in these gels. f) XRD of 0.2 and 14.1 wt% collagen gels indicated the formation of hydroxyapatite (○) in the collagen matrices. A small amount of calcite (■) was also detected remaining in 0.2 wt% collagen gels.

formed in agarose and fibroin was quite low (ca. 15 wt%), compared with chitosan and alginate (ca. 35 wt%) and a large amount was found in collagen hydrogels (ca. 75 wt%). $Ca(OH)_2$ formation was material and gel density dependent, with alginate inducing most precipitation and no $Ca(OH)_2$ formation was detected in fibroin or dense collagen gels, (Figure 1 and 3). When the samples were analyzed for the presence of ACC, we made the unexpected and highly intriguing discovery that collagen type I appears to have an innate ability to template a significant amount of stable ACC which was not dependent on the presence of $Ca(OH)_2$. Previously, using a similar crystallization system to this study, a collagen solution was reported to have a concentration-dependent effect on the morphology of calcite, by specifically inhibiting some of its crystal planes,[20] however in our study insoluble fibrillar collagen was used. The further addition of magnesium to the solution promoted the formation of vaterite,[21] however no ACC phase was noted in either previous study. Polymorph selection and orientation has also been studied using the same vapor diffusion method into gelatine xerogels enriched with polyelectrolytes. Here it was found that poly-L-aspartic acid-enriched gelatine matrices could influence the polymorph selection between calcite, vaterite and aragonite, and that uniaxial deformation of the matrices caused orientation of the crystalline components.[22] However, until now the effect of collagen in the form of hydrogels on the nucleation of ACC has not been reported. This is surprising since collagen hydrogels are mostly formed as fibrillar hydrogels. Here we have shown that collagen hydrogels are extensively mineralized with calcium carbonate, a significant proportion of which is present as a stabilized amorphous phase.

Plastic compression of collagen hydrogels facilitates control over the fibrillar density of the gel and we have previously demonstrated that a higher density corresponded to more extensive nucleation of hydroxyapatite in simulated body fluid and differences in the crystal shapes obtained.[23] Here, no such differences were noted for the formation of calcium carbonate, indicating that the microenvironment had a greater influence over calcium carbonate formation. There was a greater fraction of ACC in the 0.2 wt% gels probably due to the higher interfibrillar volume and exposed fibril surface (see Table 1, Figure 2) when compared to the 14.1 wt% counterparts. This difference was maintained upon conversion of the calcium carbonate into carbonated hydroxyapatite, resulting in a bone-like mineralization of the collagenous constructs containing nearly 80 wt% mineral for the low density collagen gel, ~55 wt% mineral for the high density gel and a volume fraction of mineralized collagen of ~0.9 for both the densities investigated after only three days of processing (Table 3). These amounts match well with those measured for human cortical bone.[24] The greater amount of mineral formed in the low density gels may be attributable to the fact that the ACC was more readily converted than that present in the high density gel. Indeed, the stability of the ACC in the low density gel appeared to be much less than that of the high density gel, since a greater proportion was lost following immersion in water.

Attempts at altering the chemical environment of the collagen gels during mineralization by the addition of soluble amino acids and elimination of magnesium ions did not significantly change the ACC content. These results suggest that a factor in the stabilization of ACC was elicited by the collagen protein and not by any amino acids in the DMEM or by a specific ionic environment. Furthermore, by blocking either the positive or negative charges present on the collagen surface ACC stabilization was prevented altogether indicating that both carbonate and calcium binding sites were required.

Biogenically, the most abundant deposition of ACC is found in the crustacean cuticle which is a composite of chitin nanofibers closely associated with proteins and reinforced with calcium carbonate.[25] The exact mechanisms of amorphous phase stabilization by the chitin fibers are not known, however certain β-chitin binding peptides have been implicated as having a role, such as n16N which stabilized synthetic ACC when applied in a silk fibroin hydrogel, ACC formed as a metastable precursor to vaterite, and it was shown that this phase may have been stable for up to 20 hours in DI water.[26] Prolonged *in vitro* stability of ACC in aqueous environments has also been shown in the continuous presence of organic molecules such as poly(propylene imine) dendrimers[27] and phytic acid,[13] where stability was achieved for up to 14 days and 3 months respectively. In both cases however, the soluble stabilising organic molecules were continuously present in the aqueous aging solution. In our study the $CaCl_2$ concentration was 100 mM (compared with 10–20 mM reported previously),[4c] since this provided sufficient mineral for analyses; this higher concentration would favor ACC formation, but do little to infer stability either during formation or subsequently.

Recently crystallization of nanoparticulate ACC was delayed by up to 20 hours by encapsulation within liposomes; in this case physical confinement was implicated as having an important role in delaying crystallization.[28] Similarly Stephens *et al.* have shown that microscale features can create a confinement effect leading to ACC stabilization.[29] In this study, the nonsoluble template maintained the stability of as formed ACC for at least six weeks in DI water free of either organic or inorganic additives. Both collagen and chitin, (with which ACC is normally found) form as nanofibers some 10–50 nm in diameter.[2] Amorphous ACC precipitates in a globular form in a range of sizes up to 1 μm in diameter (Supporting Information, Figure S1).[30] Positive radii of curvature are known to increase solubility according to the Gibbs-Thomson relation:[31]

$$\ln\left(\frac{S_c}{S_\infty}\right) = \gamma\Omega\frac{\left(R_1^{-1} + R_2^{-1}\right)}{kT} \quad (1)$$

Where S_c is the solubility of a curved solid surface, S_∞ is the solubility of a flat surface, γ is the surface energy, Ω is the atomic volume, and R_1 and R_2 are the principle radii of curvature. Close examination of the SEM images shows that the typical banding ultrastructure is absent from ACC containing collagen in which the fibril diameter also appears larger than unmineralized collagen (cf. Figure 2a,b and c,d). This suggests that ACC forms a coating on collagen nanofibers. Such a coating would essentially be a tubular shape, which has both a positive and negative radius of curvature, with the inner concave surface also having a lower energy than the ACC in solution by virtue of binding with the amphoteric collagen. The thickness of the coating can be estimated as being a minimum of 1 nm as judged by the obscuration of the collagen banding structure.

Given a fiber diameter of 50 nm and a coating thickness of 1 nm one can estimate the ACC volume to be $(26^2–25^2)/25^2$ = 8%, which is equivalent to 12 wt% since ACC has a density of 1.62 g cm^{-3}.[32] The reduction in ACC content with gel density can be accounted for by the reduction in available fiber area and also accounts for the observed upper limit of ACC content. Although the increased density of the fibers reduced the total amount of ACC, it appeared to increase the stability, possibly by increasing the (concave) contact area of ACC with collagen fibrils. Lobster and crab shells are typically 50 wt% mineral of which the majority is ACC, with some amorphous calcium phosphate, magnesium carbonate and calcite.[33] This corresponds to up to 37 vol% ACC; a 1 nm thick coating on a 10 nm chitin fibril[2] being equivalent to 31 vol%. Unlike our gels chitin fibrils are arranged parallel to one another and are organized in a hierarchical "plywood" type fashion wherein fiber density is high and ACC-fiber contact is maximized. The fibroin fibers mineralized here were approaching 1 μm in diameter and it is unlikely that ACC could form around such a large structure, except as discrete spherical nanoparticles and hence could not adopt a core-shell structure.

The mineralization of natural and reconstituted collagen has been performed using concentrated solutions of acidic polypeptides, such as poly(aspartic acid), to briefly stabilize ACC[34] and ACP.[10c] In the case of calcium carbonate mineralized collagen, the extent of mineralization was not quantified, although deposition was conducted over the period of one week. For calcium phosphate, the deposition was shown to closely resemble natural bone, although the extent of mineralization was only ~30 wt% after 7 days and the penetration of the mineral into the matrix was shown to be only about 100 μm. By taking advantage of our discovery that fibrillar type I collagen nucleated ACC, we achieved homogeneous collagen mineralization (70–80%) (comparable with cortical bone,[24]) to at least a depth of 10 mm. It is conceivable such composites could be used to fill bone defects and stimulate remodeling.

4. Conclusions

By studying the formation of ACC in a variety of biopolymers, we have made the intriguing discovery that collagen type I had a particular ability to template and stabilize ACC for prolonged periods. It would appear that the availability of a nanofibrillar amphoteric surface was key to this process. Long term stability of ACC was achieved in high density nanofibrillar collagen gels. The implication of ECM nanostructure in amorphous mineral stability is highly significant in understanding how biologically derived protective tissues can be attained by an apparently unstable and highly soluble mineral phase. Furthermore, we have demonstrated the application of this finding for the synthesis of stiff bone-like constructs which may have application as readily mineralizable hard tissue scaffold materials.

5. Experimental Section

Preparation of Biopolymer Gels and Matrices: Agarose gels were prepared by dissolving agarose (BioRad) in warm water (~60 °C) at a concentration of 2 w/v%. The agarose solution was then poured into a tissue culture dish and allowed to cool to room temperature. Following gelation the hydrogel was carefully removed from its mold. Alginate gels were prepared by dissolving sodium alginate (Fisher scientific) at a concentration of 4 w/v% in water, an equal volume of 10 mM $CaCl_2$ solution was added to crosslink the hydrogel in a tissue culture well mold. Chitosan gels were prepared by dissolving chitosan powder (100 mg, Sigma Aldrich Canada, M_v 60 000–120 000) in 2 vol% acetic acid aqueous solution (10 mL) at room temperature under gentle stirring. 1N NaOH was then added to the 2% (w/v) chitosan solution until the gelation occurred. Electrospun silk fibroin matrices were obtained as previously described.[35] Briefly, silk fibroin (SF) films were dissolved in formic acid (98 vol%, Sigma-Aldrich, Italy) at room temperature under gentle stirring. The SF solution (7.5% w/v) was transferred into a 50 ml syringe and electrospun using an *ad hoc* electrospinning system. The electrospun SF matrices were produced using the following parameters: a flow rate of 1.1 mL hr^{-1}, an electric field of 24 kV, and an electrode distance of 10 cm for a deposition time of 2 hours. The SF mats were then treated in methanol for 15 min to increase the SF crystallinity. Highly-hydrated collagen gels (0.2 wt% collagen fibrillar density, CFD) were prepared by adding dilute acid solubilized rat-tail tendon type I collagen (2.10 mg mL^{-1} in 0.6% acetic acid; First Link Ltd., U.K.) to 10 times concentrated Dulbecco Modified Eagle Medium (10× DMEM; Sigma Aldrich, Canada) at a ratio of 4:1, and adjusting the pH to 7.4 with 5 M NaOH (Fisher Scientific, Canada). Gels were prepared by casting the neutralized collagen solution in a cylindrical mold (A_{mold} = 2 cm^2, $V_{solution}$ = 2 mL) and incubating for 25 minutes at 37 °C. Dense collagen gels were prepared by increasing the fibrillar density through a plastic compression process (1 kPa for 300 s), as previously described.[36] The application of a single compression stage generated sheets of 14.1 wt% CFD. In all cases, CFD was measured by weighing the gels before and after freeze-drying (BenchTop K, VirTis, Canada). Gels (n = 5) were frozen in liquid nitrogen for 3 min followed by freeze-drying for 24 h at –105 °C and 13 mTorr.

Calcium Carbonate Mineralization: The precipitation of calcium carbonate was performed using the ammonium carbonate diffusion method in a bell jar at room temperature. Prior to mineralization, the biopolymers were washed and soaked in deionized water (18.2 MΩ) a minimum of three times until the supernatant did not form a precipitate with the addition of 1 M $AgNO_{3\ (aq)}$. Bioplymer gel samples were placed in a tissue culture well and filled with 100 mM $CaCl_{2\ (aq)}$ solution (10 mL), which was sufficient to completely immerse the biopolymers. The wells were then covered with parafilm, which was punctured thrice with a 12 G needle and placed in the bell jar. Crushed ammonium carbonate (5 g) was added to a dish, covered with parafilm, which was also punctured and then placed in the bell jar. pH measurements of the calcium chloride solution were taken at 0, 2, and 72 h reaction time using using an Oakton 1200 pH meter (Oakton Instruments,Vernon Hills, IL) with standard electrode. Samples were removed at various time points up to 72 h ours reaction for freeze drying and further analysis. Samples of calcium carbonate containing collagen gels were converted to calcium phosphate by immersion in a 200 mM aqueous solution of sodium phosphate at pH 7. To investigate the role of the chemical environment on the formation of calcium carbonate and stabilization of ACC in 0.2 wt% collagen gels, four major amino acids (AAs) of collagen (ALA, ARG, GLY, PRO, Sigma Aldrich, Canada) were added to the collagen solution at a concentration of 0.25 mg mL^{-1}. Phosphate buffered saline solution (PBS, Sigma Aldrich, Canada) replaced 10× DMEM in the collagen gelling solution to avoid the possible interference of the AAs present in the medium in the collagen mineralization process. In addition, as made gels were soaked in basic or acidic fuschine solution (10 mM, t = 2 h) to alternatively block the positive and negative charges of the protein and investigate its effects on calcium carbonate formation. At the completion of the mineralization experiments, all samples were rinsed three times in distilled water to prevent crystallization of additional calcium or ammonium salts.

Materials Characterization: Scanning electron microscopy (SEM) was carried out on sputter coated (Au-Pd) freeze dried samples using a Hitachi 4700 FE-SEM operating at an accelerating voltage of 2 kV and

10 µA beam current. X-ray diffraction (XRD) was carried out on flattened freeze dried samples using a Philips PW1710 XRD between 10 and 60° in steps of 0.02° s^{-1}.

Simultaneous thermogravimetric analysis and differential scanning calorimetry (TGA-DSC) was performed using a TA Instruments Q600 between 30 and 800 °C, at a heating rate of 10 °C min^{-1} in an air flow of 100 mL min^{-1}. MicroCT was used to analyze the distribution of minerals in the collagen gels and to calculate the volume fraction of mineralized collagen. MicroCT analysis was performed on freeze dried specimens with a SkyScan 1172 (SkyScan, Kontich, Belgium) using a 360° flat-field corrected scan at 67 kV and 175 µA, with a step size of 0.4°, a resolution of 8 µm, a large camera pixel, no filter, and 10 random movements. Volumetric reconstruction (NRecon software, SkyScan) was conducted with a beam hardening correction of 15, a ring artifact correction of 10 and an "auto" misalignment correction. A grayscale intensity range of 20-255 (8 bit images) was used in 2D analysis (software CTAn, SkyScan) to remove background noise. A previously reported protocol was used to analyze and quantify the mineralized samples.[23]

FTIR microscopy (Spectrum 400 equipped with a Spotlight 400 microscope, Perkin-Elmer, USA) was used to investigate the formation of calcium carbonate and calcium phosphate in the freeze-dried biopolymers. Three areas of 1000 × 1000 µm were scanned per sample with a spatial resolution (spot size) of 6.25 $µm^2$ and a resolution of 16 cm^{-1} at 4 scans/pixel and an IR range of 4000-700 cm^{-1}. All spectra were corrected with a linear baseline and normalized using Spotlight software (Perkin-Elmer). FTIR was also used to evaluate the formation of calcium carbonate polymorphs after the mineralization process. In particular, a protocol was developed to quantify the extent of ACC in the biopolymeric structures analyzed following methods suggested by Beniash and coworkers.[19] The ratio of the ν_2 and ν_4 absorption (874 and 713 cm^{-1}, respectively) was calculated for pure ACC, calcite and mixtures of different concentrations of the two polymorphs (Supporting Information, Figure S1b), from an area of 160 × 160 pixels representing a physical area of 1 mm^2. The mean of three measurements was calculated. The ratio was found to be linearly correlated with ACC content in calcite (R^2 = 0.99) up to a relative concentration of 70 wt% ACC. From the ν_2/ν_4 95% confidence interval, (derived using linear regression analysis in Microsoft Excel) the limit of detection was determined to be 4.2% ACC (at which point and thereafter the lower 95% confidence interval exceeded the upper confidence interval value for 100 wt% calcite, i.e. 0.0 wt% ACC) and the 95% confidence interval in ACC measurement was ±2.3% over the measured ACC range (0–15 wt%). The ν_2/ν_4 ratio was calculated from the baseline corrected spectra of collagen and fibroin, while due to the intrinsic absorption of chitosan, agarose and alginate at 874 and 713 cm^{-1}, the average absorbance of the unmineralized samples was subtracted before the calculation.

Supporting Information

Supporting Information is available from the Wiley Online Library or from the author.

Acknowledgements

D.C.B. and B.M. contributed equally to this work. The authors acknowledge grant support of NSERC and CFI. Individual members acknowledge the salary support provided by the Werner Graupe Fellowship and MEDA (BM), the Hatch Faculty Fellowship (SNN), and Canada Research Chair (JEB). Drs A. Alessandrino and G. Freddi for providing the electrospun silk fibroin matrices.

Received: December 26, 2011
Revised: April 13, 2012
Published online: May 15, 2012

[1] K. M. Rudall, W. Kenching, *Biol. Rev. Cambridge Philosophic. Soc.* **1973**, *48*, 597.
[2] H. Ehrlich, *Int. Geol. Rev.* **2010**, *52*, 661.
[3] a) M. Celerin, J. M. Ray, N. J. Schisler, A. W. Day, W. G. StetlerStevenson, D. E. Laudenbach, *Embo J.* **1996**, *15*, 4445; b) C. Wang, R. J. S. Leger, *Proc. Natl. Acad. Sci. USA* **2006**, *103*, 6647.
[4] a) F. C. Meldrum, H. Colfen, *Chem. Rev.* **2008**, *108*, 4332; b) N. Sommerdijk, G. de With, *Chem. Rev.* **2008**, *108*, 4499; c) L. B. Gower, *Chem. Rev.* **2008**, *108*, 4551.
[5] a) M. Sarikaya, C. Tamerler, A. K. Y. Jen, K. Schulten, F. Baneyx, *Nat. Mater.* **2003**, *2*, 577; b) J. Aizenberg, *Adv. Mater.* **2004**, *16*, 1295; c) D. C. Bassett, *PhD Thesis*, McGill University, Montreal **2011**; d) D. C. Bassett, M. D. McKee, J. E. Barralet, *Cryst. Growth Des.* **2011**, *11*, 803.
[6] L. Glazer, A. Shechter, M. Tom, Y. Yudkovski, S. Weil, E. D. Aflalo, R. R. Pamuru, I. Khalaila, S. Bentov, A. Berman, A. Sagi, *J. Biol. Chem.* **2010**, *285*, 12831.
[7] H. A. Lowenstam, S. Weiner, *Science* **1985**, *227*, 51.
[8] a) J. Mahamid, A. Sharir, L. Addadi, S. Weiner, *Proc. Natl. Acad. Sci. USA* **2008**, *105*, 12748; b) N. J. Crane, V. Popescu, M. D. Morris, P. Steenhuis, M. A. Ignelzi, *Bone* **2006**, *39*, 434; c) R. M. Biltz, E. D. Pellegrino, *Clin. Orthop. Rel. Res.* **1977**, 279.
[9] M. D. Grynpas, *Bone* **2007**, *41*, 162.
[10] a) A. M. Bernhardt, D. M. Manyak, K. M. Wilbur, *J. Molluscan Stud.* **1985**, *51*, 284; b) N. Watabe, A. M. Bernhardt, R. J. Kingsley, K. M. Wilbur, *Trans. Am. Micro. Soc.* **1986**, *105*, 311; c) T. T. Thula, D. E. Rodriguez, M. H. Lee, L. Pendi, J. Podschun, L. B. Gower, *Acta Biomater.* **2011**, *7*, 3158.
[11] L. Addadi, S. Raz, S. Weiner, *Adv Mater.* **2003**, *15*, 959.
[12] J. Aizenberg, G. Lambert, L. Addadi, S. Weiner, *Adv. Mater.* **1996**, *8*, 222.
[13] A. W. Xu, Q. Yu, W. F. Dong, M. Antonietti, H. Colfen, *Adv. Mater.* **2005**, *17*, 2217.
[14] A. Sato, S. Nagasaka, K. Furihata, S. Nagata, I. Arai, K. Saruwatari, T. Kogure, S. Sakuda, H. Nagasawa, *Nat. Chem. Biol.* **2011**, *7*, 197.
[15] D. C. Bassett, L. M. Grover, F. A. Muller, M. D. McKee, J. E. Barralet, *Adv. Funct. Mater.* **2011**, *21*, 2968.
[16] R. Chester, H. Elderfield, *Sedimentology* **1967**, *9*, 5.
[17] A. V. Radha, T. Z. Forbes, C. E. Killian, P. Gilbert, A. Navrotsk, *Proc. Natl. Acad. Sci. USA* **2010**, *107*, 16438.
[18] T. Sakae, H. Mishima, Y. Kozawa, R. Z. LeGeros, *Connect. Tissue Res.* **1995**, *33*, 193.
[19] E. Beniash, J. Aizenberg, L. Addadi, S. Weiner, *Proc. R. Soc. B* **1997**, *264*, 461.
[20] F. H. Shen, Q. L. Feng, C. M. Wang, *J. Cryst. Growth* **2002**, *242*, 239.
[21] Y. Jiao, Q. Feng, X. Li, *Mater. Sci. Eng., C* **2006**, *26*, 648.
[22] G. Falini, *Int. J. Inorg. Mater.* **2000**, *2*, 455.
[23] B. Marelli, C. E. Ghezzi, J. E. Barralet, S. N. Nazhat, *Soft Matter* **2011**, *7*, 9898.
[24] W. S. S. Jee, in *Cell and tissue biology: A textbook of histology*, (Ed: L. Weiss), Urban & Schwarzenberg, Baltimore, MD **1988**, Ch. 7.
[25] A. Al-Sawalmih, C. H. Li, S. Siegel, P. Fratzl, O. Paris, *Adv. Mater.* **2009**, *21*, 4011.
[26] E. C. Keene, J. S. Evans, L. A. Estroff, *Cryst. Growth Des.* **2010**, *10*, 5169.
[27] J. Donners, B. R. Heywood, E. W. Meijer, R. J. M. Nolte, C. Roman, A. Schenning, N. Sommerdijk, *Chem. Commun.* **2000**, 1937.
[28] C. C. Tester, R. E. Brock, C. H. Wu, M. R. Krejci, S. Weigand, D. Joester, *CrysEngComm* **2011**, *13*, 3975.
[29] C. J. Stephens, S. F. Laden, F. C. Meldrum, H. K. Christenson, *Adv. Funct. Mater.* **2010**, *20*, 2108.
[30] L. Brecevic, *J. Cryst. Growth* **1989**, *98*, 504.
[31] G. Cao in *Nanostructures & nanomaterials: synthesis, properties & applications*, Imperial College Press, London **2004**, Ch. 2.

[32] a) J. Liu, S. Pancera, V. Boyko, A. Shukla, T. Narayanan, K. Huber, *Langmuir* **2010**, *26*, 17405. b) J. Bolze, B. Peng, N. Dingenouts, P. Panine, T. Narayanan, M. Ballauff, *Langmuir* **2002**, *18*, 8364.
[33] F. Bobelmann, P. Romano, H. Fabritius, D. Raabe, M. Epple, *Thermochim. Acta* **2007**, *463*, 65.
[34] M. J. Olszta, D. J. Odom, E. P. Douglas, L. B. Gower, *Connect. Tissue Res.* **2003**, *44*, 326.
[35] A. Alessandrino, B. Marelli, C. Arosio, S. Fare, M. C. Tanzi, G. Freddi, *Eng. Life Sci.* **2008**, *8*, 219.
[36] R. A. Brown, M. Wiseman, C. B. Chuo, U. Cheema, S. N. Nazhat, *Adv. Funct. Mater.* **2005**, *15*, 1762.